Structural Studies of Lysyl-tRNA Synthetase: Conformational Changes Induced by Substrate Binding†

Silvia Onesti,*,‡ Gianluigi Desogus,‡ Annie Brevet,§ Josiane Chen,§ Pierre Plateau,§ Sylvain Blanquet,§ and Peter Brick‡

Biophysics Section, Blackett Laboratory, Imperial College, London SW7 2BZ, U.K., and Laboratoire de Biochimie, Ecole Polytechnique, 91128 Palaiseau Cedex, France

Received June 28, 2000; Revised Manuscript Received August 10, 2000

ABSTRACT: Lysyl-tRNA synthetase is a member of the class II aminoacyl-tRNA synthetases and catalyses the specific aminoacylation of $tRNA^{Lys}$. The crystal structure of the constitutive lysyl-tRNA synthetase (LysS) from *Escherichia coli* has been determined to 2.7 Å resolution in the unliganded form and in a complex with the lysine substrate. A comparison between the unliganded and lysine-bound structures reveals major conformational changes upon lysine binding. The lysine substrate is involved in a network of hydrogen bonds. Two of these interactions, one between the α-amino group and the carbonyl oxygen of Gly 216 and the other between the carboxylate group and the side chain of Arg 262, trigger a subtle and complicated reorganization of the active site, involving the ordering of two loops (residues 215−217 and 444−455), a change in conformation of residues 393−409, and a rotation of a 4-helix bundle domain (located between motif 2 and 3) by 10°. The result of these changes is a closing up of the active site upon lysine binding.

The translation of genetic information into protein sequences is mediated by adaptor molecules (transfer RNA) which recognize a triplet on the messenger RNA through a complementary region called an anticodon and carry a covalently attached amino acid corresponding to that triplet in the genetic code. Aminoacyl-tRNA synthetases are the ubiquitous enzymes that are responsible for the specific aminoacylation of transfer RNA. The selectivity in their recognition of both the amino acid to be activated and the cognate tRNA is a crucial step in the fidelity of the translation of the genetic code, since the pairing of the mRNA codon with the tRNA anticodon is independent of the nature of the amino acid carried.

The aminoacyl-tRNA synthetases differ widely in both size and oligomeric state but carry out a similar overall two-step reaction: in the first step, ATP is used to activate the amino acid through the formation of an aminoacyl-adenylate intermediate, while in the second step the amino acid is transferred to either the 2′OH or 3′OH of the terminal adenosine of the tRNA molecule. Despite the lack of significant overall homology between the twenty synthetases with different amino acid specificities, the identification of a few conserved motifs has revealed that the enzymes can be grouped into two separate classes, class I and class II (*1*), with each class containing 10 members. At the same time, results from X-ray crystallography studies have shown how each class is characterized by a similar architecture of the catalytic domain. Three-dimensional structures are now available for many of the class I [TyrRS[1] (*2*), GlnRS (*3*), MetRS (*4*, *5*), TrpRS (*6*), GluRS (*7*), ArgRS (*8*), IleRS (*9*), LeuRS (*10*)] and class II enzymes [SerRS (*11*) AspRS (*12*), LysRS (*13*), AsnRS (*14*), ThrRS (*15*), ProRS (*16*), HisRS (*17*), PheRS (*18*), GlyRS (*19*)].

Lysyl-tRNA synthetase is a member of the class II synthetases. The enzymes in this class are mostly dimers and share a common catalytic domain containing three conserved sequence motifs. In addition to the catalytic core they include a variety of accessory domains which are added onto the common scaffold in a modular fashion. Often present is a domain which is involved in the recognition of the tRNA anticodon, which in most systems is an important determinant of tRNA identity. Class II synthetases can therefore be further subdivided into subfamilies characterized by a relatively higher sequence homology within the catalytic domain, by similar topology of the anticodon recognition domains and by a similar location of the additional accessory domains. In subfamily IIb, which comprises LysRS, AspRS, and AsnRS, the anticodon binding domain is located at the N-terminus of the amino acid sequence and is built around a β-barrel whose topology has been described as the oligonucleotide-binding (OB) fold (*20*). In all three members of this subfamily a large insertion occurs at a similar position (between motif 2 and motif 3) in the catalytic domain, but the topology of this insertion domain is highly variable, being different not only for different enzymes, such as LysRS and AspRS, but also for enzymes with the same amino acid specificity belonging to

† This work was supported by a Wellcome Trust Grant (Grant 050370). G.D. is a recipient of a Marie Curie Research Training Fellowship. Synchrotron data collection at Hamburg was supported by a EU/TMR LSF grant.

* To whom correspondence should be addressed. E-mail: s.onesti@ic.ac.uk. Phone: 020-75947647. Fax: 020-75890191.

‡ Biophysics Section.

§ Laboratoire de Biochimie.

[1] LysRS, lysyl-tRNA synthetase; aaRS, amino-acyl tRNA synthetase.

10.1021/bi001487r CCC: $19.00
Published on Web 09/26/2000

different organisms,such as for prokaryotic and yeast AspRS.

In *Escherichia coli* two different proteins displaying lysyl-tRNA synthetase activity are coded by genes [*lysS* and *lysU* (*21*)] which are subjected to different regulation: LysS is expressed constitutively under normal growth conditions, while LysU is the product of a relatively silent gene, which is overexpressed under certain physiological conditions such as high temperature, anaerobiosis, low external pH, or the presence of leucine (*21*−*24*). The two proteins share 88% sequence identity and have very similar enzymatic properties. However, in the presence of saturating substrate concentrations, LysS is about twice as active as LysU in the ATP−PP_i exchange reaction as well as in $tRNA^{Lys}$ aminoacylation, while the dissociation constant of the LysU:lysine complex is 8-fold smaller than that of the LysS:lysine complex (*25*). As a result LysU is relatively less sensitive than LysS to the presence of cadaverine, a decarboxylation product of lysine which behaves as a competitive inhibitor of lysine binding and shows similar affinities for both enzymes. Cadaverine is produced at the expenses of lysine in several stress responses, including most of the conditions which induce *lysU* expression. A comparison between the thermostabilities of LysU and LysS also shows that at 42 °C the half-life of LysU activity is twice that of LysS, in agreement with the fact that *lysU* expression accompanies the adaptation of the bacterium to heat shock (*25*).

The three-dimensional structure of LysU with a lysine bound to the active site has been determined to 2.8 Å resolution by the isomorphous replacement method (*13*, *26*). Higher resolution data (2.1 Å) were subsequently obtained from frozen crystals belonging to a related hexagonal crystal form (*27*). Crystals of LysU require lysine to grow, and a lysine molecule is found tightly bound to the active site, even when crystals are soaked for a long time in a lysine-free solution. This requirement for lysine suggested that the protein may undergo a conformational change on binding the substrate, but crystals of LysU in the absence of the amino acid ligand have not been obtained.

The crystal structures of *Thermus thermophilus* LysRS complexed with either the modified *E. coli* $tRNA^{Lys}$ or the *T. thermophilus* $tRNA^{Lys}$ transcript have also been published (*28*). In both complexes only the tRNA anticodon is well ordered. Additional data were presented for LysRS crystals diffracting to only 3.8 Å resolution, cocrystallized with both the tRNA and a nonhydrolysable lysyl-adenylate analogue.

Here we report the crystal structure of the unliganded lysyl-tRNA synthetase LysS and compare it with the lysine-bound structure. The comparison reveals major conformational changes involving the ordering of two loops and the reorientation of the insertion domain, which is located between motifs 2 and 3. The changes can be described as a closing up of the active site upon lysine binding.

EXPERIMENTAL PROCEDURES

Protein Expression and Purification. LysS was purified from strain PAL2103UKTR [F^-Δ(*lac-pro*)*gyrA rpoB metBargE*(Am) *ara supF* Δ*lysU::kan srl-300*::Tn*10 recA56*] transformed by plasmid PXLysKS1 ($lysS^+$) (*25*). Cells were grown overnight in 4 L of 2xTY medium containing 100 μg/mL ampicillin and 0.5 mM IPTG. Sonication of the cells, removal of nucleic acids, ammonium sulfate precipitation, and hydroxylapatite chromatography were performed as described before (*25*), except that a 3.8 × 19 cm hydroxylapatite column was used. The protein sample was brought to 70% ammonium sulfate saturation and centrifuged for 30 min at 12000*g*. After dialysis against 20 mM Tris-HCl buffer (pH 7.8) containing 10 mM 2-mercaptoethanol, 0.1 mM EDTA, and 0.1 mM PMSF, the sample was applied onto a Q-Sepharose column (2.5 × 12 cm, Pharmacia) equilibrated in the same buffer. Elution was carried out at 180 mL/h through a 1.5 L linear gradient from 0 to 500 mM KCl in the same buffer. A total of 250 mg of LysS protein were obtained and kept as an ammonium sulfate (70%) precipitate. Prior to crystallization the precipitate was sedimented, dissolved in 20 mM Tris-HCl, pH 8.0, and dialyzed against 20 mM Tris-HCl (pH 8.0) and 10 mM 2-mercaptoethanol.

Table 1

	unliganded	lysine-bound
cell parameters		
a, *b* (Å)	181.9	181.8
c (Å)	92.5	93.1
data collection statistics		
synchrotron	Hamburg	Daresbury
beamline	Desy BW7B	SRS 9.6
wavelength (Å)	0.88	0.87
maximum resolution (Å)	2.7	2.7
no. of measurements	108 202	87 419
independent reflections	25 416	25 113
completeness (outer shell) (%)	99.6 (99.2)	99.2 (99.1)
$R_{merge(outer\ shell)}$ (%)[a]	5.6 (26.0)	7.1 (22.2)
intensity/σ (outer shell)	8.7 (2.9)	6.0 (3.2)
refinement statistics		
R-factor (%)[b]	25.2	22.8
R_{free} (%)	30.8	29.7
rms bond length (Å)	0.012	0.008
rms bond angle (deg)	1.8	1.4

[a] $R_{merge} = \sum_h\sum_i|I_i(h) - \langle I(h)\rangle|/\sum_h\sum_i I_i(h)$, where $I_i(h)$ is the *i*th measurement of reflection *h* and $\langle I(h)\rangle$ is the weighted mean of all measurements of *h*. [b] *R*-factor $=\sum_h|F_{obs} - F_{calc}|/\sum_h F_{obs}$, where F_{obs} and F_{calc} are the observed and calculated structure factors.

Crystallization and Data Collection. Crystals of unliganded LysS were grown by vapor diffusion using the hanging drop technique. The protein was concentrated to about 20 mg/mL using an Amicon micro-concentrator in 20 mM Tris-HCl (pH 8.0) and 10 mM 2-mercaptoethanol; 10 mM $MgCl_2$ was added prior to crystallization. The hanging drops contained equal volumes of the protein solution and a reservoir solution containing 0.1 M Hepes buffer at pH 7.5, 46−50% saturated ammonium sulfate solution, 2−4% poly(ethylene glycol) 400, 15−20% glycerol. Large hexagonal bypiramid-shaped crystals grew at both 4 and 18 °C: often many small crystals appeared as clusters, but occasionally a few rather large crystals could be obtained, reaching dimensions of up to 1 mm × 1 mm × 0.6 mm. The crystals diffract to at least 2.7 Å resolution and belong to space group $P\bar{6}22$, with cell dimensions $a = b = 182$ Å, $c = 93$ Å (Table 1). The volume of the unit cell is consistent with a monomer in the asymmetric unit and 68% of solvent.

Crystals of LysS are weakly diffracting and susceptible to X-ray radiation damage so that all data collection was carried out at cryogenic temperature. Crystals were frozen in a stream of nitrogen gas at 100 K using an Oxford Cryosystem. The crystals were grown in 15−20% glycerol so that no transfer to a harvesting solution containing a cryoprotectant was necessary. Native data to 2.7 Å resolution

were collected at DESY (Hamburg, Germany) on the wiggler beam line BW7B using a MarResearch imaging plate system. Diffracted intensities for a crystal soaked for 30 min in a solution containing 5 mM lysine were measured at the Synchrotron Radiation Source (Daresbury, U.K.). The images were evaluated using a modified version of MOSFLM (A. Leslie), and the CCP4 program suite (*29*) was used for data reduction and analysis. A summary of the data collection statistics is given in Table 1.

Molecular Replacement Solution and Refinement. The structure was solved by molecular replacement with the program AMoRe (*30*), using the coordinates of the 2.1 Å resolution complex between LysU and lysine (*27*). The search model consisted of the molecular dimer with the substrate lysine and solvent molecules removed and the side chains of residues which were different between LysS and LysU set to alanines. Cross-rotation function calculations (performed with data between 20 and 5 Å resolution for the native crystal) gave a clear peak with a height of 20σ. Translation function calculations also yielded an unambiguous solution having a correlation coefficient between calculated and observed Patterson vectors of 51.7% and a *R*-factor of 45.0%, with the dimer positioned in such a way as to place the molecular 2-fold axis on a crystallographic 2-fold axes in the hexagonal unit cell. This solution was improved by rigid-body fitting giving a final *R*-factor of 43.8% for data between 20 and 5 Å resolution.

The crystallographic refinement was carried out using the program X-PLOR (*31*). A random sample containing 5% of the data was excluded from the refinement and the agreement between calculated and observed structure factors for those reflections (R_{free}) was used to monitor the course of the refinement (*32*). The model was restrained with Engh and Huber stereochemical parameters (*33*). Low resolution data to 20 Å were included and a bulk solvent correction applied throughout the refinement procedure.

Although the molecular replacement solution was straightforward, the refinement of the structure presented some difficulties. The initial rounds of refinement using the diffraction data for the unliganded LysS crystals failed to lower the R_{free} below 40%. Changes in the model indicated that some conformational changes were occurring, but various attempts at modeling the changes by breaking the model into fragments and carrying out rigid-body refinement at very low resolution to increase the radius of convergence, were unsuccessful. Simulated annealing procedures also failed to model the changes.

An alternative approach was therefore taken by refining the structure of LysS in its lysine-bound form, which was found to more closely resemble the LysU:lysine complex used as a starting model. The refinement of the LysS:lysine complex proceeded smoothly, leading to a final model with an *R*-factor of 22.8% (Table 1). The final model for the LysS:lysine complex includes residues 11−153 and 161−502, 152 water molecules, and a lysine bound to the active site.

The coordinates of the LysS:lysine complex were then used to refine the unliganded form using the same methodology described above. Many cycles of rigid-body refinement were carried out at very low resolution (data between 20 and 8 Å resolution) by initially breaking the model into large domains or subdomains. Higher resolution data were gradually incorporated in the refinement and the model broken into smaller fragments. The course of the refinement was monitored by using the free *R*-factor. Rounds of positional and temperature refinement using all data from 20 to 2.7 Å were alternated with manual rebuilding using the interactive computer graphics program O (*34*). Simulated annealing omit maps have been calculated to verify the interpretation of the electron density map. The final model has good geometry and is refined to an *R*-factor of 25.2% against all data (Table 1). No electron density is present for the 10 N-terminal amino acids, the 2 C-terminal amino acids, for residue 269 and the regions enclosed between residues 154−160, 215−217, and 444−455.

The coordinates of the unliganded and lysine-bound models have been deposited in the Protein Data Bank (Brookhaven), with accession numbers 1BBW and 1BBU, respectively.

RESULTS AND DISCUSSION

Overall Structure. The overall structure of lysyl-tRNA synthetase LysS is very similar to LysU, as expected given the very high sequence homology shared by the two enzymes. The protein is a homodimer, with the two subunits related by a crystallographic 2-fold axis and an extended dimeric interface spanning the entire length of the molecule. Each monomer has a molecular mass of 58 kDa, and is made up of 504 amino acid residues which fold into two clearly separate regions (Figure 1A): a smaller N-terminal domain built around a β-barrel, which is responsible for the recognition of the tRNA anticodon, and a larger C-terminal domain which contains the active site and consists of an extended antiparallel β-sheet surrounded by long helices, with a topology characteristic of the catalytic domain of class II synthetases. A short segment connecting the N-terminal and C-terminal domains (residues 154−160) was not visible in the electron density.

A comparison of the LysRS crystal structure with the structures of other class II synthetases enables a conserved core to be identified (shown in green in Figure 1). An insertion occurs in class IIb synthetases between helix H9 and strand B5 which results in an additional β-strand (B4) being added to the central β-sheet (Figure 1B). With the exception of strand B4, the topology of the insertion domain is different in the various class IIb molecules for which three-dimensional structures are available. Strands D1 and D2 in LysRS are replaced by a loop in the *T. thermophilus* AspRS (*35*), an α-helix in the yeast AspRS structure (*12*) and two short helices in the *T. thermophilus* AsnRS (*14*), while the LysRS four-helix bundle (H10, H11, H12, and H13) becomes a $\beta\alpha\beta$ split motif domain in the prokaryotic AspRS, a helix-turn-helix in the same enzyme from *S. cerevisiae* and two helices in AsnRS. In the crystal structure of the archaeal AspRS (*36*) there is also an insertion between H9 and B5, but the eighth strand (B4 in LysRS) present in all other class IIb structures is missing. This is therefore a region in which a large variety of structural modules are found, which is different not only in the various members of the same IIb subfamily, but also in proteins from different organisms with the same amino acid specificity.

Active Site. Aminoacyl-tRNA synthetases catalyze a two-step reaction which involves the activation of the amino acid as an adenylate and the successive transfer of the amino acid

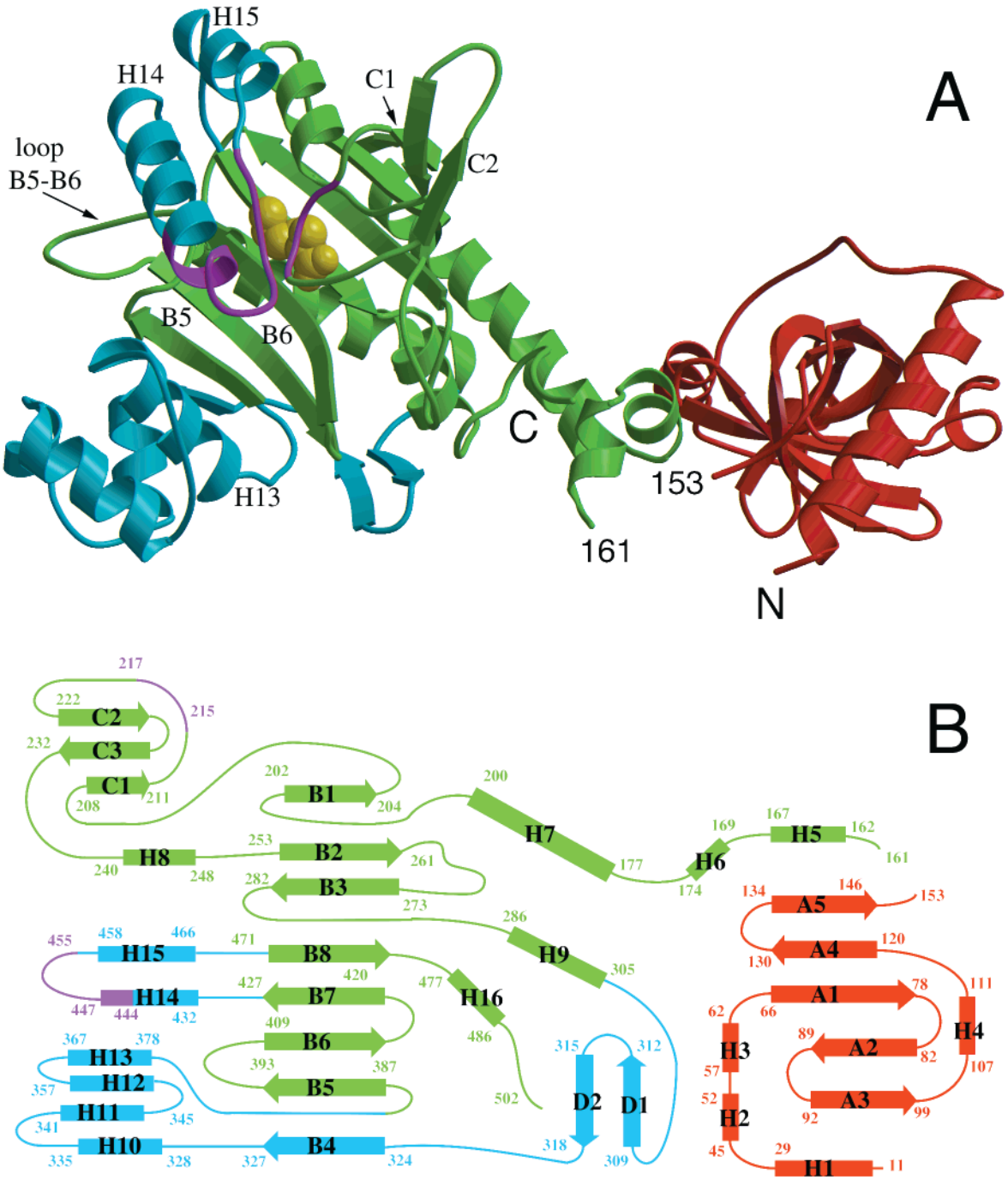

FIGURE 1: Structure of a monomer of LysS in a complex with the lysine substrate. (A) Ribbon representation of the monomer viewed down the molecular 2-fold axis with the lysine substrate drawn in yellow using a space-filling representation. The N-terminal anticodon-binding domain is shown in red. Within the larger domain which contains the catalytic site, the conserved core which is common to all class II aminoacyl-tRNA synthetases is shown in green, while the secondary structure elements which are characteristic of the lysyl-tRNA synthetase structure are in blue. The two loops (215−217 and 444−455) which are disordered in the uncomplexed LysS structure are indicated in magenta. Selected secondary structure elements are labeled. (B) A schematic illustration of the topology of a LysS monomer: β-strands are represented as arrows and helices as rods. The secondary structure elements are color coded as in Figure 1A.

moiety onto the ribose of the 3′ terminal adenosine residue of the cognate tRNA. The active site must therefore recognize the amino acid, ATP, and the acceptor end of the tRNA.

In the crystal structure of the LysS:lysine complex, the lysine substrate is recognized through a network of interactions involving a number of charged and polar side chains (Figure 2). Tyr 280, Glu 428, and Glu 240 hydrogen bond to the ϵ-amino group; Asn 424 and Arg 262 interact with the α-carboxylate, while Glu 278 and Glu 240 stabilize the position of the α-amino group. In addition to these interactions, a hydrogen bond is formed between the free α-NH_3^+ of the lysine and the main-chain carbonyl of Gly 216. When the structure is compared with that of the LysU:lysine complex, all of the interactions made by the lysine are virtually identical in the two enzymes.

An unusual feature of the unliganded LysS structure is the presence, on one of the helices of the insertion domain (H13), of three glutamate residues (Glu 373, Glu 376, Glu 380) whose carboxylate moieties are within hydrogen-bonding distances. These acidic residues are conserved in

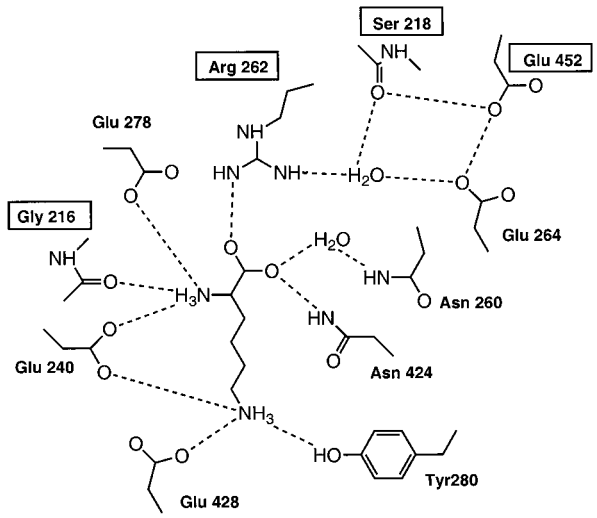

FIGURE 2: Schematic representation of the active site of the LysS:lysine complex, indicating the potential hydrogen bonding pattern responsible for the recognition of the lysine substrate. The residues which are disordered in the absence of the substrate are shown in boxes.

the LysU sequence (Asp 376 substituting Glu 376). There is no evidence for positive ions mediating the interaction (despite the presence of Mg^{2+} in the crystallization medium) and the carboxylate oxygens are within 2.7 and 2.9 Å from one another (Figure 3). This arrangement clearly implies an unusual chemical environment, able to shift their pK_a so that at least two of the side chains are protonated at neutral pH. In both the LysRS:lysine complexes the same residues "open up" so that the carboxylate side chains are further apart. Helix H13 faces the active site, being approximately located where the CCA acceptor stem is expected to bind.

It is interesting to note that a similar interaction involving two glutamate side chains has been found in the vicinity of the active site of the unliganded GlyRS (*19*) and it has been suggested that the field generated by this unusual configuration might be important in attracting the free α-amino group of the amino acid substrate. In this context lysine may be particularly subjected to such an electrostatic field because of both the α- and ϵ-amino groups present on the molecule.

Conformational Changes upon Lysine Binding. Crystals of LysS were obtained in the absence of the lysine substrate and when the protein was incubated with lysine prior to crystallization experiments, the pattern of solubility changed dramatically. In particular, under the conditions in which the unliganded enzyme yielded crystals, the lysine-bound form came out of solution as a heavy precipitate. Such a behavior strongly suggested that amino acid binding induces a conformational change. However, we were able to soak unliganded LysS crystals in a solution containing lysine, determine the lysine-bound structure and compare it to the unliganded LysS in order to analyze the conformational changes which occur on lysine binding.

When the catalytic domains for the unliganded and lysine-bound structures are superposed through manual iteration selecting all residues within the cutoff of 1.5 Å, 266 α-carbon positions, out of the 340 residues in the C-terminal domain, overlap (Figure 4, panels A and B). Most of the differences result from a reorientation of the helices H10 to H13 of the insertion domain. A superposition of the 4-helix bundle (residues 328−378) can be achieved by applying a pure rotation of 10° so that the helices move toward the active site in the lysine-bound form.

Whereas in the unliganded enzyme the regions between residues 215−217 and 444−455 are completely disordered, in the lysine-bound structure both segments of polypeptide chain show well-defined electron density. The 215−217 loop (located between β-strands C1 and C2) adopts a conformation that brings the main-chain oxygen of Gly 216 within hydrogen-bonding distance (2.7 Å) from the free α-amino group of the substrate lysine (Figure 4C). The polypeptide between strands B7 and B8 folds into two helices (residues 432−447 and 458−466) connected by a long loop. This region is located between the C1−C2 loop on one side, with residues 453−455 within a few angstroms from residues 216 and 217, and the helix H13 of the insertion domain on the other side. There are no direct interactions between the helices H14 and H15 and either the 215−217 loop or helix H13, and all of the hydrogen bonds are through water molecules.

There is no electron density for the side chain of the conserved motif 2 arginine (Arg 262) in the unliganded form. On lysine binding this residue takes an ordered conformation and forms a hydrogen bond with the α-carboxylate of the substrate lysine (Figure 4C). The conformational change that occurs on lysine-binding results in the formation of some additional hydrogen bonds. A well-defined water molecule makes a bridge between the guanidinium group of Arg 262 and the carboxylate of Glu 264, which interacts with Glu 452 on the loop between H14 and H15. The same water molecule is hydrogen bonded to the main-chain oxygen of residue 218. All of these interactions are lost when lysine is not bound to the enzyme active site.

The long loop which connects strands B5 and B6 (393−409) also shows significant changes in the lysine-bound structure, with most of the Cα positions shifted by about 2 Å as compared to the unliganded LysS. In particular the ψ angle of Pro 398 changes from −130° (in the unliganded form) to −10° (in the lysine-bound form) and the side chain of Leu 399, disordered in the unliganded form, adopts an ordered conformation. The side chain of Phe 426 rotates in the presence of the substrate, assuming a different conformation so that the aromatic ring is wedged between the side chain of the lysine substrate and Leu 399. In the lysine-bound structure, Pro 398, Leu 399, Phe 439, and Met 454 pack to form an hydrophobic cluster, with the side chain of Met 454 adjacent to the main chain of Gly 217. The region between 393 and 395 packs against the 4-helix bundle, with the side chain of Glu 395 making a number of key hydrogen bonds with the main-chain atoms of residues 366−369 in the insertion domain (H13).

Thus, to summarize, on lysine binding the gain of two hydrogen bonds (one between the α-NH_3^+ of lysine and the carbonyl oxygen of residues 216 and the other between the α-carboxylate group of the amino acid substrate and the guanidinium moiety of Arg 262) triggers a subtle and complicated network of interactions which, through the ordering of the regions between residues 215−217 and 444−455 and the adjustment of the torsion angles of residues located in loop 393−409, results in a large conformational change around the active site with the entire region between residues 328−378 rotating by more than 10°. All these

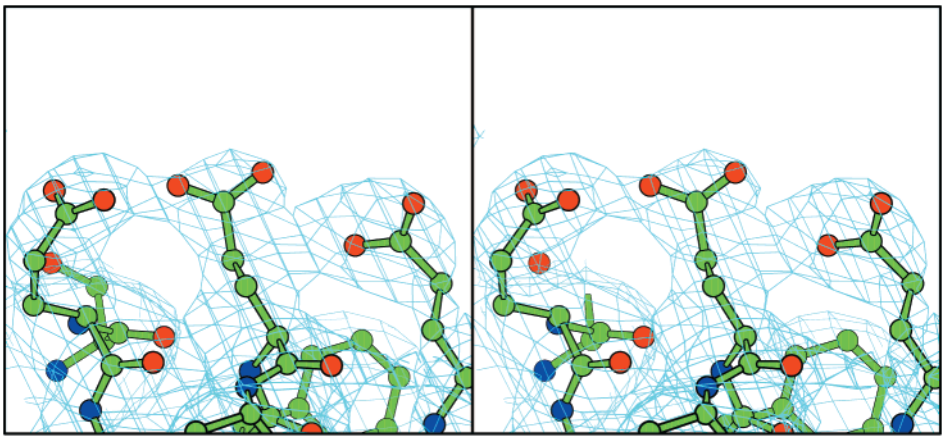

FIGURE 3: Stereodiagram of a section of the final electron density map for the unliganded LysS structure showing the close interaction between Glu 373, Glu 376, and Glu 380, located on helix H13. The oxygens of the carboxylates are within hydrogen bonding distance, implying an unusual chemical environment able to shift their pK_a, so that at least two side chains are protonated. In the crystal structure of the LysS:lysine complex the three carboxylates move apart. The map was calculated using all data between 20 and 2.7 Å resolution, and contoured at the 1σ level.

changes close up the active site around the substrate.

The existence of two states for lysyl-tRNA synthetase with different affinity for lysine has been postulated in the case of a LysS mutant (T207A) which binds lysine in a highly cooperative fashion (*37*). Threonine 207 is located at the subunit interface and immediately precedes the absolutely conserved Pro 208 in motif 1. It is tempting to speculate that the two conformations we observe in the absence and presence of the substrate lysine are the two postulated states. On the other hand, there is no evidence for cooperativity toward lysine binding in the wild-type enzyme and, when we compare the dimer interface in the lysine-bound and unliganded LysS there are no obvious differences that could explain how the binding of the substrate to one subunit could affect the conformation of the other subunit.

A similar movement has been observed in the structure of *T. thermophilus* LysRS cocrystallized in the presence of the cognate tRNA (*28*). The structure of the enzyme:tRNA complex has been solved to 2.9 Å resolution; additional data to 3.8 Å have been presented for a ternary complex with a lysyl-adenylate analogue. Although the low resolution of the data does not allow a detailed interpretation at the atomic level, the main features of the induced conformational change are consistent with our observations.

Conformational changes associated with substrate binding have been reported for a number of other class II aminoacyl-tRNA synthetases. In the AsnRS structure (*14*) the binding of an analogue of the adenylate intermediate is linked to the ordering of the loop that is topologically equivalent to the C1−C2 loop and the concerted movement of two helices equivalent to H14 and H15. In the archaeal AspRS structure (*36*) more direct evidence of the importance of the conformational changes involving the loop equivalent to our C1−C2 (which has been described as the flipping loop) is presented. In one of the two subunit of the dimeric molecule, crystal-packing interactions lock the loop in an open conformation, generating an asymmetry in the two halves of the molecule. This translates into a functional asymmetry, with the free monomer being able to bind the amino acid substrate and forming the aminoacyl-adenylate intermediate, while the locked active site does not bind the aspartic acid substrate and is therefore inactive.

Comparison with LysU. Neither the biological role of LysU with respect to LysS, nor the differential regulation of the two LysRS genes are completely understood. The higher affinity for lysine shown by LysU makes it less sensitive to inhibition by cadaverine, a lysine-degradation product which accumulates in bacteria grown under physiological conditions similar to those that induce *lysU* expression (*25*).

When the crystal structure of LysU and LysS complexed with lysine are compared, most of the features described above are very similar in the two enzymes, but the movement of the insertion domain toward the active site is less marked in the LysS:lysine complex than in the LysU:lysine complex. The insertion domain of the unliganded LysS structure needs to be rotated by 10° to reach the position assumed in the LysS:lysine complex and by 14° for the LysU:lysine complex. Despite this difference, all the interactions between the insertion domain and the rest of the protein are virtually identical in the two complexes.

This slightly different orientation of the insertion domain may be due to the fact that LysU has been cocrystallized in the presence of lysine, while LysS crystals have been grown in the absence of any substrate and then soaked into lysine-containing solutions. The insertion domain is in fact involved in crystal contacts in the unliganded LysS structure, with the region between residues 329 and 338 (which includes helix H10) interacting with residues 30−31 and 404−405 of a symmetry related molecule. These interactions are either hydrophobic or hydrogen bonds mediated by ordered water molecules. When lysine binds to LysS some of these interactions are retained, although through a different network of water molecules. Therefore the LysS crystal packing may not be compatible with the completion of the conformational changes which normally follow lysine binding, and only a smaller rotation of the insertion domain can occur without disrupting the crystal lattice.

Another possibility would be that the differences we observe are intrinsic properties of the LysU and LysS enzymes and reflect their different specificities for lysine, so that the larger conformational change upon lysine binding seen in LysU correlates with the recovery of more free energy and a tighter binding. It is very difficult to identify which residues might be responsible for these differences. Only 56

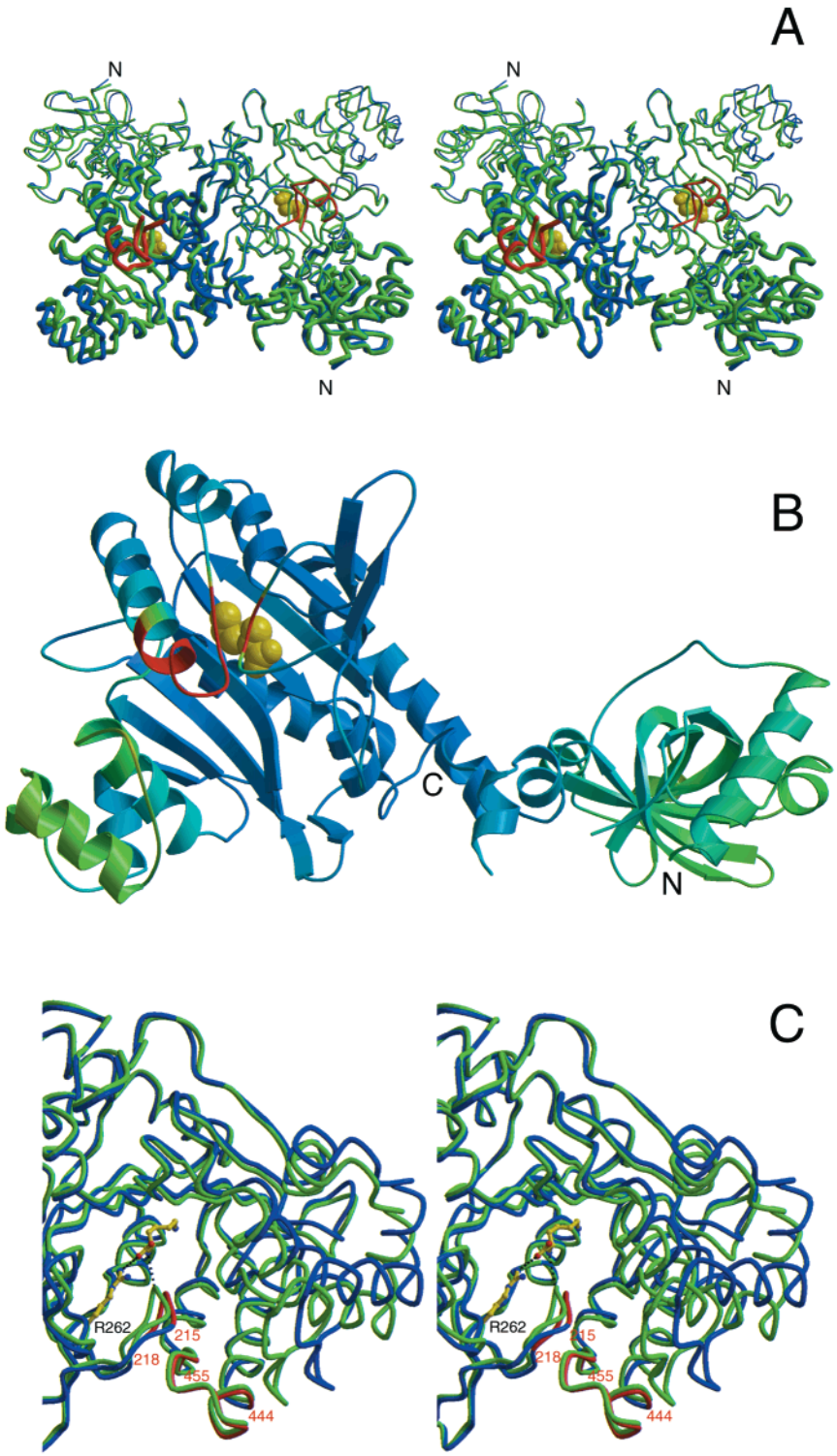

FIGURE 4: Conformational changes that occur on binding of the lysine substrate. (A) Convergent stereodiagram showing a superposition of the LysS dimer backbone in the absence and presence of the lysine substrate. The molecule is in the same orientation as Figure 1A, with the dimer axis perpendicular to the page. The lysine-bound enzyme is shown in green. The unliganded LysS is shown in blue with the loop that becomes ordered on lysine binding modeled in red. The two subunits in the dimer are distinguished by the use of thick and thin lines. A space-filling model of the lysine substrate is shown in yellow. (B) A ribbon representation of a monomer of LysS colored according to the rms differences between the α-carbon positions in the unliganded and lysine-bound enzymes, when the core of the catalytic domains are superimposed. The structure is colored from blue to green, where in blue are shown the regions for which the rms differences are less than 1.5 Å, while in green are shown the regions that move up to 6 Å. The two loops that are disordered in the unliganded structure are colored in red. A space filling model of the lysine is shown in yellow. (C) A close up of the active site showing a stereo superposition of the lysine-bound (green) and unliganded (blue) LysS. In the unliganded structure the loops that are disordered (residues 215−218 and 444−455) have been modeled for the sake of clarity and are shown in red. A model for the lysine substrate and the motif 2 Argr 262 as seen in the lysine-bound structure are shown in yellow. The hydrogen bonds between the α-amino group of the lysine and the carbonyl of residue 216 and between the lysine α-carboxylate and the guanidinium group of Arg 262 are shown as dashed lines. The formation of these two hydrogen bonds cause the ordering of the regions 215−218 and 444−455 and the reorientation of the 4-helix bundle, here shown on the right-hand side of the picture.

amino acid residues of 504 are different in the two lysyl-tRNA synthetases: most of these residues are located on the surface of the protein and are exposed to the solvent and none is involved in lysine binding. A few residues that could have a subtle effect on the conformational changes observed are located on helix H14 or on strand D2.

Reorientation of the N-Terminal Domain. When the catalytic domains of the unliganded and lysine-bound LysS structures are overlapped onto the catalytic domain of the LysU:lysine complex, rigid-body rotations (of 3 and 6°, respectively) need to be applied to optimally superpose the N-terminal domains.

There has been considerable discussion about the functional relevance of the relative orientations of the N-terminal and C-terminal domains in the various structures available for both the AspRS and the LysRS system. In some cases these differences amounts to a rotation of 20° and are consistent with a change triggered by tRNA binding, since both the AspRS:$tRNA^{Asp}$ complex (*12*) and the LysRS:$tRNA^{Lys}$ complex (*28*) have a more open conformation of the anticodon binding domain than the corresponding isolated enzymes (*13*, *35*). At the same time, both the AspRS structures are more open than the LysRS structures, suggesting that there might be an intrinsic difference in the two enzymes. One of the problems in interpreting the significance of this movement is the fact that all the studied structures (uncomplexed *E. coli* LysRS, *T. thermophilus* LysRS:$tRNA^{Lys}$ complex, uncomplexed *T. thermophilus* AspRS, and yeast AspRS:$tRNA^{Asp}$ complex) are from different organisms and have homologous but different sequences, precluding a direct comparison.

In the comparison between the two *E. coli* LysRSs, the fact that the relative orientation of the N-terminal domain in the unliganded structure is halfway between that observed for the two lysine bound structure (LysU:lysine complex and LysS:lysine complex) suggests that the extent and direction of the movement is not correlated with the presence of the amino acid substrate. The observed movement indicates a degree of flexibility, so that the relative orientation of the two domains can be locked in one particular conformation by subtle changes possibly due to different crystallization conditions.

Implication for ATP and tRNA Binding. The crystal structures of LysU in the presence of ATP, the lysyl-adenylate intermediate, and the nonhydrolyzable ATP analogue AMP−PCP have been recently determined (*27*). As in all class II synthetases, one of the key interactions observed in these complexes is that between the ATP α-phosphate and the guanidinium group of the motif 2 arginine (Arg262). Since the ordering of the side chain of Arg 262 is one of two interactions responsible for the changes upon lysine binding in LysS, we have tried to verify whether binding of ATP alone could cause a similar conformational change, but attempts to soak ATP into the unliganded LysS crystals have been unsuccessful.

Despite the overall structural similarity between LysRS and AspRS, only a very crude model for the LysRS:$tRNA^{Lys}$ complex can be built by using the known three-dimensional structure of the yeast AspRS:$tRNA^{Asp}$ complex (*12*). In particular the modeling of the interactions made by the CCA acceptor stem is hindered by the fact that most of the structural differences between the two enzymes are clustered in the acceptor stem binding site region. When the atomic coordinates for the catalytic domain of AspRS and LysRS are superposed and the position of the CCA extrapolated from the $tRNA^{Asp}$ model, there are obvious steric clashes between A76 and the main-chain atoms of the loop C1−C2 in the LysRS model. Moreover, the different conformation assumed by the insertion domain and the helices H14 and H15 makes the LysRS active site considerably less exposed to the solvent compared to that of AspRS. These are the same regions which are involved in the conformational change triggered by lysine binding. It is very possible that these regions undergo an additional conformational change upon tRNA binding.

Indeed, a similar situation has been observed in the case of the AspRS system (D. Moras, personal communication). Yeast $tRNA^{Asp}$ binds to *E. coli* AspRS but is not aminoacylated: when the crystal structure for both the productive complex (i.e., yeast $tRNA^{Asp}$/yeast AspRS) and nonproductive complex (yeast $tRNA^{Asp}$/*E. coli* AspRS) are compared, the main difference in the protein involves the loop which corresponds to the C1−C2 loop in LysRS. In the nonproductive complex, this loop assumes a conformation which sterically interferes with the putative binding site for the adenosine A76 of the tRNA molecule. In the productive complex the loop flips into a conformation which allows the positioning of A76 close to the phosphate of the aminoacyl-adenylate and packs tightly against the CCA acceptor stem. In both AspRS and LysRS the amino acid sequence of the C1−C2 loop consists entirely of small amino acids (Gly, Ala, Ser), which probably account for the observed flexibility; moreover larger side chains would sterically interfere with the binding of the CCA acceptor stem.

A similar switch involving another loop (the motif 2 loop) has been observed in the structure of *T. thermophilus* SerRS, upon tRNA binding (*38*). It has been speculated that these conformational changes are important to ensure the correct dynamics of the reaction, and in particular the ordered passage through the amino acid activation and tRNA transfer steps.

ACKNOWLEDGMENT

We thank the staff at the Synchrotron Radiation Source, Daresbury Laboratory and at DESY, Hamburg.

REFERENCES

1. Eriani, G., Delarue, M., Poch, O., Gangloff, J., and Moras, D. (1990) *Nature 347*, 203−206.
2. Brick, P., Bhat, T. N., and Blow, D. M. (1989) *J. Mol. Biol. 208*, 83−98.
3. Rould, M. A., Perona, J. J., Söll, D., and Steitz, T. (1989) *Science 246*, 1135−1142.
4. Mechulam, Y., Schmitt, E., Maveyraud, L., Zelwer, C., Nureki, O., Yokoyama, S., Konno, M., and Blanquet, S. (1999) *J. Mol. Biol. 294*, 1287−1297.
5. Sugiura, I., Nureki, O., Ugaji-Yoshikawa, Y., Kuwabara, S., Shimada, A., Tateno, M., Lorber, B., Giege, R., Moras, D., Yokoyama, S., and Konno, M. (2000) *Struct. Folding Des. 8*, 197−208.
6. Doublié, S., Bricogne, G., Gilmore, C., and Carter, C. W., Jr. (1995) *Structure 3*, 17−31.
7. Nureki, O., Vassylyev, D. G., Katayanagi, K., Shimizu, T., Sekine, S., Kigawa, T., Miyazawa, T., Yokoyama, S., and Morikawa, K. (1995) *Science 267*, 1958−1965.

8. Cavarelli, J., Delagoutte, B., Eriani, G., Gangloff, J., Moras, D., and Arnez, J. G. (1998) *EMBO J. 18*, 5438−5448.
9. Nureki, O., Vassylyev, D. G., Tateno, M., Shimada, A., Nakama, T., Fukai, S., Konno, M., Hendrickson, T. L., Schimmel, P., and Yokoyama, S. (1998) *Science 280*, 578−582.
10. Cusack, S., Yaremchuk, A., and Tukalo, M. (2000) *EMBO J. 19*, 2351−2361.
11. Cusack, S., Berthet-Colominas, C., Härtlein, M., Nassar, N., and Leberman, R. (1990) *Nature 347*, 249−255.
12. Ruff, M., Krishnaswamy, S., Boeglin, M., Poterszman, A., Mitschler, A., Podjarny, A., Rees, B., Thierry, J. C., and Moras, D. (1991) *Science 252*, 1682−1689.
13. Onesti, S., Miller, A. D., and Brick, P. (1995) *Structure 3*, 163−176.
14. Berthet-Colominas, C., Seignovert, L., Härtlein, M., Grotli, M., Cusack, S., and Leberman, R. (1998) *EMBO J. 17*, 2947−2960.
15. Sankaranarayanan, R., Dock-Bregeon, A. C., Romby, P., Caillet, J., Springer, M., Rees, B., Ehresmann, C., Ehresmann, B., and Moras, D. (1999) *Cell 97*, 371−381.
16. Cusack, S., Yaremchuk, A., Krikliviy, I., and M, T. (1998) *Structure 6*, 101−108.
17. Arnez, J. G., Augustine, J. G., Moras, D., and Francklyn, C. S. (1997) *Proc. Natl. Acad. Sci. U.S.A. 94*, 7144−7149.
18. Mosyak, L., Reshetnikova, L., Goldgur, Y., Delarue, M., and Safro, M. G. (1995) *Nat. Struct. Biol. 2*, 537−547.
19. Logan, D. T., Mazauric, M.-H., Kern, D., and Moras, D. (1995) *EMBO J. 14*, 4156−4167.
20. Murzin, A. G. (1993) *EMBO J. 12*, 861−867.
21. Lêvèque, F., Plateau, P., Dessen, P., and Blanquet, S. (1990) *Nucleic Acid Res. 18*, 305−312.
22. Clark, R. L., and Neidhardt, F. C. (1990) *J. Bacteriol. 172*, 3237−3243.
23. Lêvèque, F., Gazeau, M., Fromant, M., Blanquet, S., and Plateau, P. (1991) *J. Bacteriol. 173*, 7903−7910.
24. Gazeau, M., Delort, F., Dessen, P., Blanquet, S., and Plateau, P. (1992) *FEBS Lett. 300*, 254−258.
25. Brevet, A., Chen, J., Lêvèque, F., Blanquet, S., and Plateau, P. (1995) *J. Biol. Chem. 270*, 14439−14444.
26. Onesti, S., Theoclitou, M. E., Pernilla, E., Wittung, L., Miller, A. D., Plateau, P., Blanquet, S., and Brick, P. (1994) *J. Mol. Biol. 243*, 123−125.
27. Desogus, G., Todone, F., Brick, P., and Onesti, S. (2000) *Biochemistry 39*, 8418−8425.
28. Cusack, S., Yaremchuk, A., and Tukalo, M. (1996) *EMBO J. 15*, 6321−6334.
29. Collaborative Computational Project Number 4. (1994) *Acta Crystallogr., Sect. D 50*, 760−763.
30. Navaza, J. (1994) *Acta Crystallogr., Sect. A50*, 157−163.
31. Brünger, A. T., Kuriyan, J., and Karplus, M. (1987) *Science 235*, 458−460.
32. Brünger, A. T. (1992) *Nature 355*, 472−474.
33. Engh, R. A., and Huber, R. (1991) *Acta Crystallogr., Sect. A 47*, 392−400.
34. Jones, T. A., Zou, J.-Y., Cowan, S. W., and Kjeldgaard, M. (1991) *Acta Crystallogr., Sect. A 47*, 110−119.
35. Delarue, M., Poterszman, A., Nikonov, S., Garber, M., Moras, D., and Thierry, J.-C. (1994) *EMBO J. 13*, 3219−3229.
36. Schmitt, E., Moulinier, L., Fujiwara, S., Imanaka, T., Thierry, J.-C., and Moras, D. (1998) *EMBO J. 17*, 5227−5237.
37. Commans, S., Blanquet, S., and Plateau, P. (1995) *Biochemistry 34*, 8180−8189.
38. Cusack, S., Yaremchuk, A., and Tukalo, M. (1996) *EMBO J. 15*, 2834−2842.

BI001487R